MATERIALS PHYSICS AND MECHANICS RESEARCH ARTICLE

Submitted: June 10, 2026 **Revised: July 21, 2026** **Accepted: July 27, 2026**

Stress-induced martensite aging accompanied ω-phase precipitation in NiFeGaCo single crystals

E.E. Timofeeva ✉, E.Yu. Panchenko, N.Yu. Surikov, M.V. Zherdeva, Yu.I. Chumlyakov

National Research Tomsk State University, Tomsk, Russia

✉ timofeeva_katie@mail.ru

ABSTRACT

The effect of ω-phase particles precipitated prior to or during stress-induced martensite aging (SIM-aging) on the two-way shape memory effect (TWSME), reversible strain, thermal hysteresis and martensite formation temperature has been established in $Ni_{47.5}Fe_{15}Ga_{27.5}Co_{10}$ single crystals. The experiment was conducted on single-phase quenched single crystals. In contrast, SIM-aging was accompanied by the precipitation of ω-phase particles in oriented $L1_0$-martensite, and on heterophase single crystals, where ω-phase was previously precipitated in unloaded $L2_1$-austenite, whereas SIM-aging was not accompanied by particle precipitation. The TWSME characterized by optimal parameters: a high reversible strain of up to 4 %, narrow thermal hysteresis (15 – 30 K), and high temperatures (M_S^* up to 417 K) obtained in heterophase $Ni_{47.5}Fe_{15}Ga_{27.5}Co_{10}$ single crystals, in which ω-phase particles precipitated before SIM-aging in the austenitic $L2_1$-phase, compared with quenched single crystals, where nanoscale ω-phase particles precipitated in the oriented $L1_0$-martensite during SIM-aging.

KEYWORDS

martensitic transformation • stress-induced martensite aging • two-way shape memory effect • ω-phase particles Heusler alloys • NiFeGaCo

Funding. *This work was supported by the Russian Science Foundation (grant No. 24-19-00242).*

Citation: Timofeeva EE, Panchenko EYu, Surikov NYu, Zherdeva MV, Chumlyakov YuI. Stress-induced martensite aging accompanied ω-phase precipitation in NiFeGaCo single crystals. *Materials Physics and Mechanics*. 2026;54(4): 1 – 10.
http://dx.doi.org/10.18149/MPM.5442026_1

Introduction

Over the last ten years, the influence of stress-induced martensite aging (SIM-aging) on the functional properties of shape memory alloys has been actively investigated [1 – 8]. This technique has been successfully applied to control the temperatures of martensitic transformations (MTs), induce a two-way shape memory effect (TWSME), and modify superelasticity (SE) [1 – 8]. The result of SIM-aging is the chemical stabilization of oriented martensite through the diffusion-driven redistribution of point defects and different type of atoms in accordance with a martensite symmetry. Therefore, SIM-aging leads to the TWSME in stress-free thermal cycles, a change in the martensite start temperature and thermal hysteresis, which has been extensively studied in Heusler alloys (NiFeGa(Co), CoNiGa, NiMnGa) [1 – 8]. In contrast, chemical and mechanical stabilization of martensite appears as a consequence of the martensite fixation by defects (for example, during plastic deformation), and leads to a broadening of the hysteresis and a decrease in the reversible strain TWSME [9,10].

© E.E. Timofeeva, E.Yu. Panchenko, N.Yu. Surikov, M.V. Zherdeva, Yu.I. Chumlyakov, 2026.
Publisher: Peter the Great St. Petersburg Polytechnic University
This is an open access article under the CC BY-NC 4.0 license (https://creativecommons.org/li-censes/by-nc/4.0/)

Typically, SIM-aging does not involve the precipitation of secondary phases and occurs at temperatures below the particle precipitation range. This is caused by the particle precipitation at higher temperatures (above 623–673 K), where a stress-induced MT is accompanied by significant plastic deformation and SIM aging is not performed. In the study [11], the new chemical composition of $Ni_{47.5}Fe_{15}Ga_{27.5}Co_{10}$ (at. %) alloy was discovered. The precipitation of nanoscale ω-phase particles has a positive effect on the properties of $Ni_{47.5}Fe_{15}Ga_{27.5}Co_{10}$ alloys: an increase in the martensite yield strength and a widening of the SE temperature range. Important, that the temperature range for the ω-phase precipitation overlaps with the SE range: in the quenched $Ni_{47.5}Fe_{15}Ga_{27.5}Co_{10}$ single crystals, the ω-phase precipitation temperature T_ω = 488 K is only 65 K higher than the starting temperature of the SE range, 423 K. This combination of parameters opens up new possibilities for SIM-aging with simultaneous precipitation of ω-phase particles. However, it is also possible to precipitate ω-phase particles prior to SIM-aging through aging in the stress-free austenite, and then conduct the SIM-aging in a heterophase alloy without additional precipitation. This raises the question of how particle precipitation (prior to or during SIM-aging) will affect the TWSME, reversible strain, thermal hysteresis and the martensite formation temperature, which determines the relevance of this work. Thus, the aim is to investigate the TWSME after SIM-aging in quenched and heterophase [001]-oriented $Ni_{47.5}Fe_{15}Ga_{27.5}Co_{10}$ (at. %) single crystals.

Materials and Methods

The $Ni_{47.5}Fe_{15}Ga_{27.5}Co_{10}$ (at. %) single crystals were grown using the Bridgman method; 3 × 3 × 6 mm³ samples were cut with the compression axis aligned along the high-strength [001] direction. Along this direction, SIM-aging was performed, and TWSME was studied. SIM-aging was performed on the single crystals after the following heat treatments:

1. a high-temperature annealing at 1448 K for 1 h, followed by water quenching (single-phase quenched single crystals);
2. after quenching, the aging was conducted in the stress-free austenite at 523 K for 1 h (heterophase single crystals).

The heat treatment conditions were selected based on [11,12]: the quenched single crystals contained no secondary phases, whereas the aged heterophase single crystals contained nanoscale particles of the ω-phase. The MT temperatures (M_s, M_f, A_s, A_f) were obtained by measuring the temperature dependence of the electrical resistivity. Differential scanning calorimetry (DSC) was used to determine the ω-phase transition temperatures, employing a NETZSCH DSC 404 F1 calorimeter during heating/cooling cycles with a rate of 20 K/min. A Universal Keyence VHX 2000 complex with a Linkam TST350 testing frame for in-situ cooling/heating was used for metallographic observations. During the analysis of experimental data, the measurement errors of strain (± 0.3 %), temperature (± 2 K), and stress (± 2 MPa) were taken into account.

SIM-aging was performed on dilatometer IMRS-1 as follows. A compressive stress of 500 MPa was applied to a sample at room temperature T_K in martensite state, inducing a reorientation of the martensite variants to one oriented martensite. Then the loaded sample was heated (with a rate of 20 K/min) until the aging temperature T_{SIM} and kept in

martensite under stress for 1 h (Fig. 1). Aging stress (500 MPa) and aging time (1 h) were constant, but the aging temperature T_{SIM} was varied for different samples.

In single-phase quenched single crystals, SIM-aging was performed only at temperatures from 503 to 533 K, which is above the ω-phase precipitation temperature, T_ω = 488 K (Fig. 1(a)). The method described above allowed to precipitate the ω-phase in stress-induced martensite and exclude a precipitation in stress-free austenite phase. For preliminary aged (at 523 K) a heterophase single crystal, which has already contained the ω-phase particles, the temperature for the additional ω-phase precipitation T_ω = 585 K is much higher, than T_{SIM}, which was variated from 398 to 533 K (Fig. 1(b)). Therefore, there was no additional precipitation of the ω-phase during SIM-aging in heterophase single crystal. After SIM-aging, the reverse MT was realized by two possible variants (marked by circled 1 and 2). First was realized when unloading was enough for the reverse MT and the complete strain recovered. Second variant was observed when unloading didn't induced complete strain recovery and heating (with a rate of 20 K/min) was required for reverse MT (Fig. 1(b)).

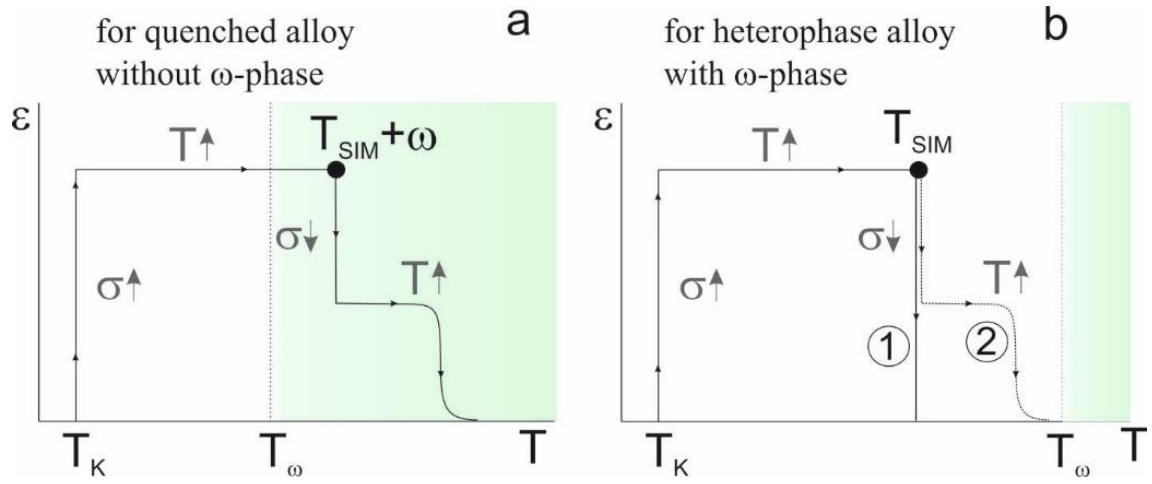


Fig. 1. The scheme of SIM-aging process and followed reverse MT: (a) SIM-aging accompanied with ω-phase precipitation in quenched crystals; (b) SIM-aging without ω-phase precipitation in heterophase single crystals

Before and after SIM-aging TWSME was studied on each sample using a dilatometer to obtain the $\varepsilon(T)$ curves during stress-free cooling/heating with a rate of 10 K/min. The measurement error was ± 0.3%. The TWSME was measured under the minimum possible applied stress of 0.5–0.7 MPa necessary to fix the sample position.

Results and Discussion

Figure 2 shows the results of calorimetric studies and endothermic peaks associated with the formation of the ω-phase in quenched and heterophase $Ni_{47.5}Fe_{15}Ga_{27.5}Co_{10}$ single crystals. In the quenched single crystals (black curve in Fig. 2), the onset of the ω-phase precipitation peak is T_ω = 488 K, and the area is 7.6 J/g. Evidence for the precipitation of ω-phase particles in the $L2_1$ matrix at these temperatures in $Ni_{47.5}Fe_{15}Ga_{27.5}Co_{10}$ single crystals was observed by TEM and presented in [11].

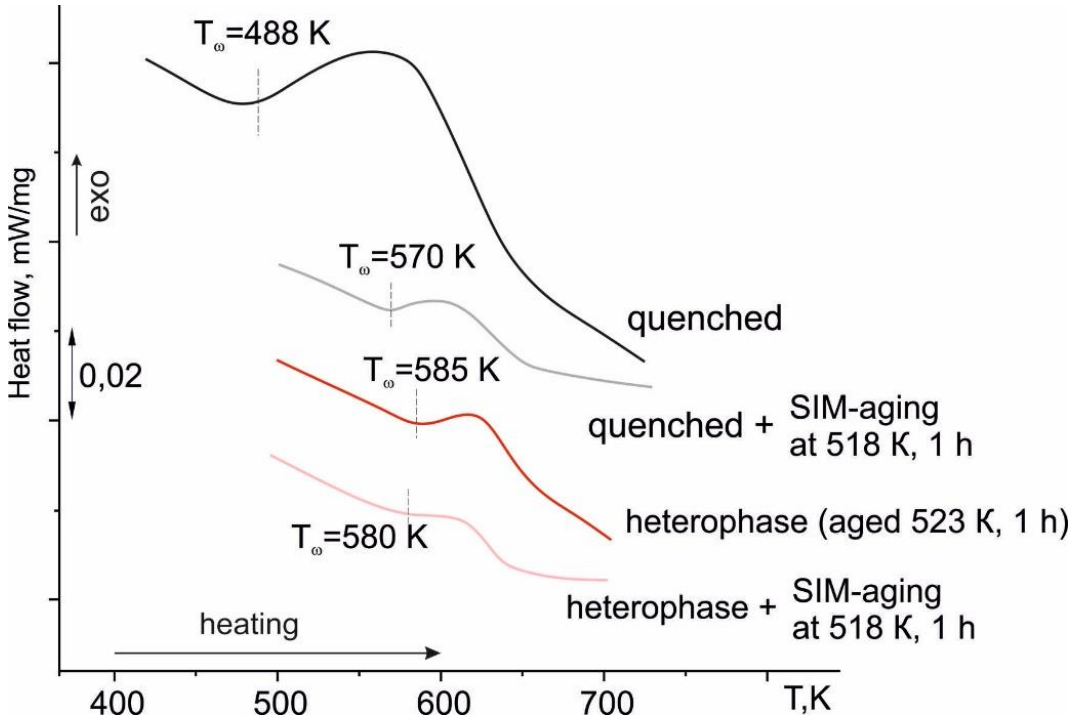


Fig. 2. DSC exothermic curves during heating for single crystals after quenching (black curve), after quenching and SIM-aging (grey curve), after aging at 573 K, 1h (red curve), after aging at 573 K, 1h and SIM-aging (pink curve)

In [11,13,14], it was shown that after aging and particle precipitation, the heat peak corresponding to the second phase decreases and shifts to a higher temperature range. This occurs because the structural and chemical instabilities of the B2-phase, which led to particle precipitation, are partly removed, and subsequent calorimetric studies result in a smaller precipitation of the ω-phase. Consequently, the calorimetric tests can serve as indirect evidence of particle precipitation.

In the quenched single crystals, SIM-aging was performed only at temperatures above the ω-phase particle precipitation temperature, T_ω = 488 K. Following SIM-aging at 518 K for 1 h, the subsequent heating shows that the peak of ω-phase decreases significantly from 7.6 to 1.0 J/g, while the precipitation temperature increases to T_ω = 570 K (Fig. 2, grey curve). These values become close to those of heterophase single crystals that have been pre-aged in austenite at 523 K (red curve in Fig. 2): the peak area is 1.4 J/g, and the temperature T_ω = 585 K. Consequently, it can be concluded that particle precipitation occurs in quenched single crystals during SIM-aging.

In the heterophase single crystals, SIM-aging was conducted only at temperatures from 398 to 533 K below the ω-phase particle precipitation temperature, T_ω = 585 K. Therefore, in these single crystals, the heat peak associated with ω-phase precipitation remains unchanged (area and temperature T_ω) after SIM-aging at 518 K (pink curve in Fig. 2). Consequently, it can be assumed that the ω-phase particles do not dissolve during SIM-aging and there was no additional particles precipitation.

Another indirect evidence of particle precipitation during the SIM-aging process in the quenched single crystals is the increase in the martensite yield strength, measured at 300 K. The effects of dispersion hardening from nanoscale particles lead to a significant increase in mechanical properties compared to single-phase alloys [15,16]. In [11], it was

found that the martensite yield strength was 1025 MPa in the quenched $Ni_{47.5}Fe_{15}Ga_{27.5}Co_{10}$ single crystals. Aging in austenite at 523 K for 1 h increases the martensite yield strength to 1640 MPa due to the precipitation of the ω-phase (Fig. 3(a)). As can be seen from Fig. 3(b), if quenched single crystals were subjected to SIM-aging at 518 K for 1 h under a load of 500 MPa, the martensite yield strength increases to practically the same value (1570 MPa) as after aging in stress-free austenite.

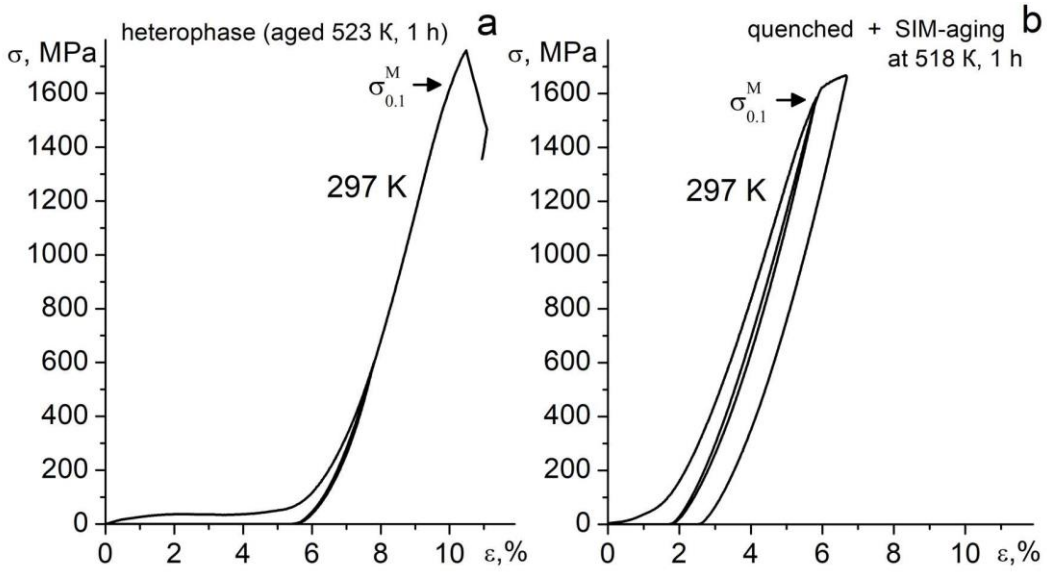


Fig. 3. The $\sigma(\varepsilon)$ curves illustrating the martensite yield strength in alloys containing ω-phase particles: (a) heterophase single crystals (aging in stress-free austenite at 523 K for 1 h); (b) quenched single crystals after SIM-aging at 518 K for 1 h at 500 MPa

Figures 4 and 5 show the TWSME curves obtained during stress-free cooling/heating cycles, before and after SIM-aging in the quenched and heterophase single crystals, as a function of the aging temperature, T_{SIM}. Before SIM-aging, the reversible strain does not exceed 0.1 % (Fig. 4). During SIM-aging under compression with a stress of 500 MPa applied along the [001] direction, the twinned variant of $L1_0$-martensite stabilized, in accordance with [8]. It has been repeatedly shown that martensite contains $<111>_{L10}$ nanotwins [17,18]. All SIM-aging regimes lead to the stabilization of the $L1_0$-martensite and excluded the TWSME (Fig. 5).

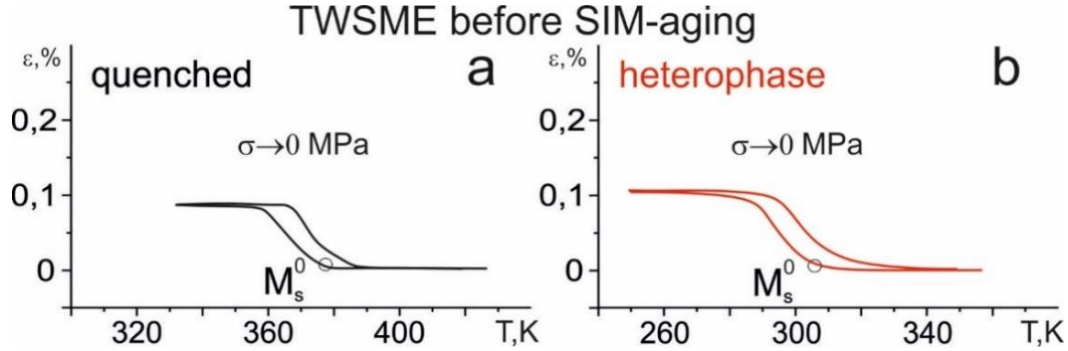


Fig. 4. Stress-free cooling/heating cycles before SIM-aging in the quenched single crystals (a) and heterophase single crystals (b)

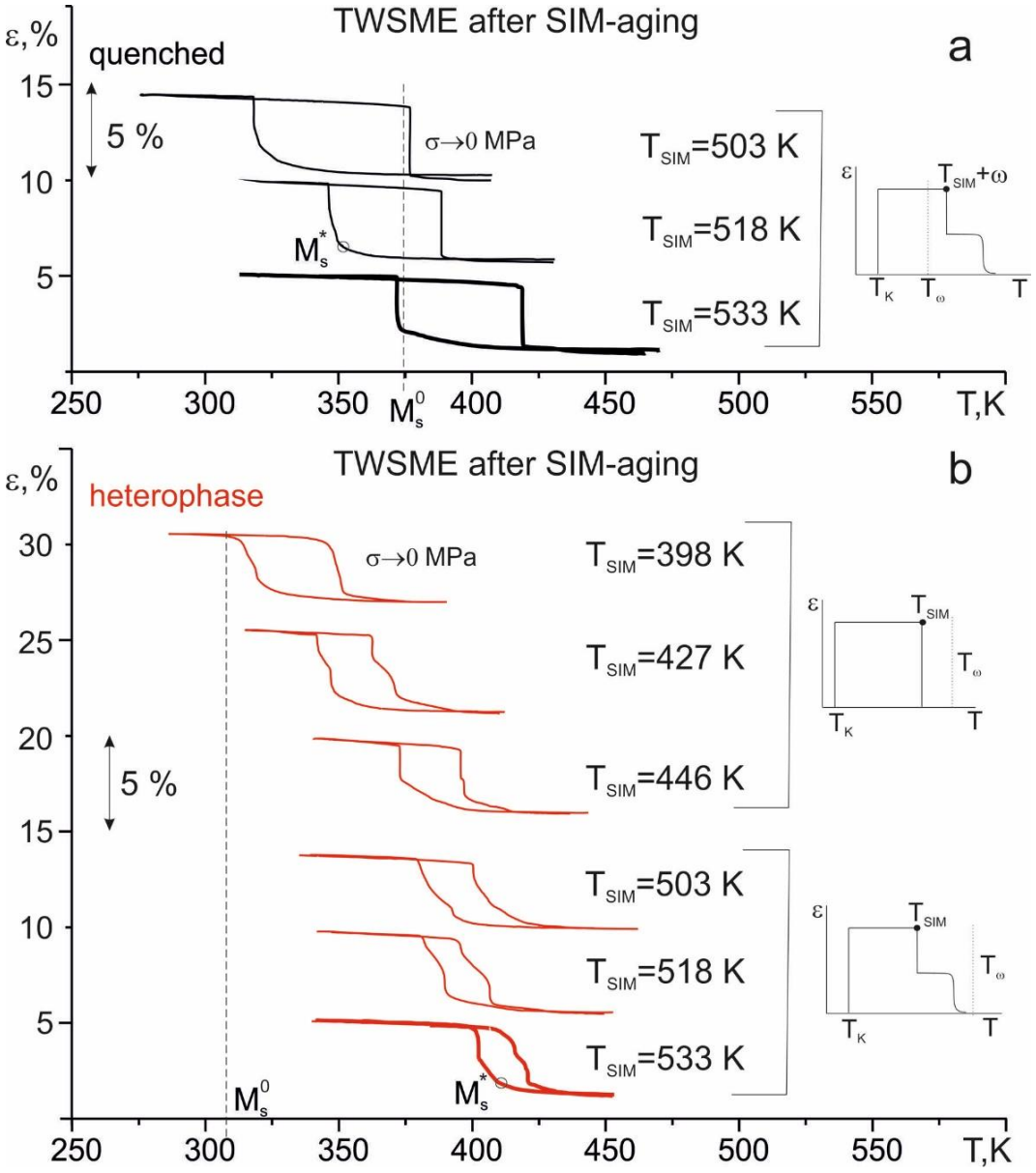


Fig. 5. TWSME in stress-free cooling/heating cycles following SIM-aging in the quenched single crystals (a) and heterophase single crystals (b)

The TWSME strain is practically independent of the initial state, the SIM-aging temperature and the precipitation of the nanoscale ω-phase, and amounts to 3.7–4.1 %. In contrast, the temperature of oriented martensite formation, M_S^*, and the thermal hysteresis, Δ*T*, strongly depend on the SIM-aging temperature and the initial state (quenched or heterophase).

All TWSME curves obtained after SIM-aging in quenched single crystals with simultaneous particle precipitation (Fig. 5(a)) are characterised by a wide thermal hysteresis of 45–60 K, which is attributed to high frictional forces acting on the interphase boundary. In this case, the MT proceeds in two stages: first, a slow accumulation of strain (0.5 %) over a temperature range of 10–15 K, followed by a rapid transformation stage within a narrow range of 1–3 K, during which the strain increases to 3.7–4.0 %. Such MT is typically observed when the system must overcome a barrier to

the formation of a large volume fraction of martensite, which requires significant overcooling during both the forward and reverse phase transformations. This results in the wide hysteresis of TWSME. In this case, reversible energy is practically not stored during the transformation [19,20], which proceeds with a single interphase boundary (Fig. 6(a)). The explosive behaviour of MT has been observed in other shape memory alloys, for example [21], and can be used in actuator applications [22].

In heterophase single crystals, where particles were precipitated only before SIM-aging (Fig. 5(b)), the TWSME curves are characterized by narrow thermal hysteresis, $\Delta T = 15–30$ K, which is 2–3 times smaller than in quenched single crystals after SIM-aging ($\Delta T = 45–60$ K). At the same time, the intervals of the forward and reverse MT are wider, amounting to 10–15 K. Consequently, another phase transition mechanism is observed in this case: the formation of oriented martensite occurs with multiple phase boundaries that move gradually, leading to the accumulation of significant elastic energy – the driving force of the reverse MT (Fig. 6(b)).

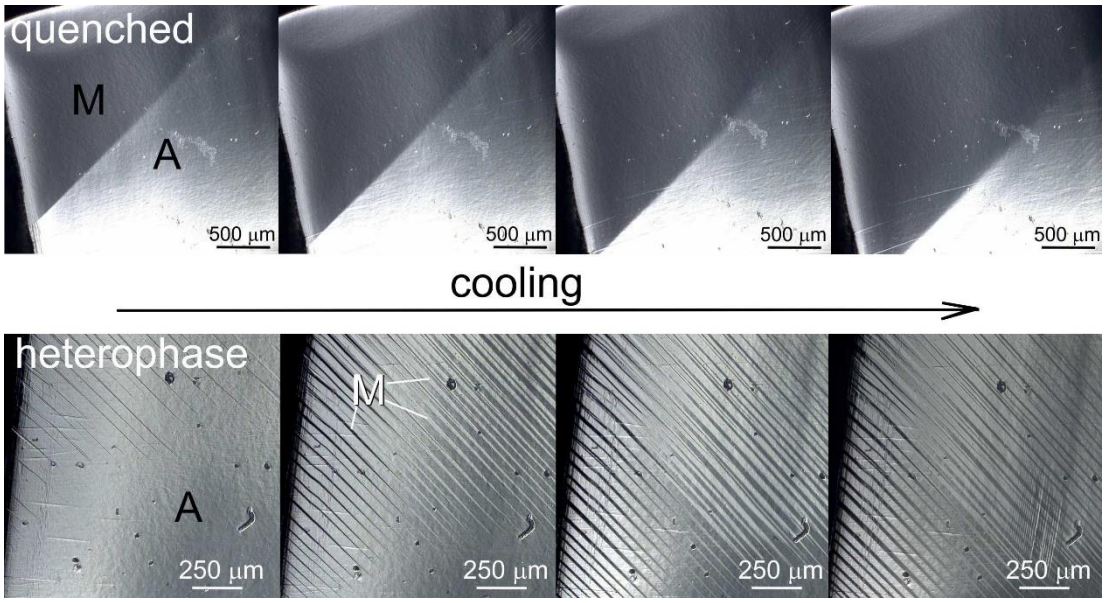


Fig. 6. Optical metallography of the surface of single crystals during cooling: (a) quenched single crystals after SIM-aging at 533 K; (b) heterophase single crystals after SIM-aging at 533 K

In [23,24], it was shown that this difference in the TWSME curves is determined by the twin structure of the stabilized $L1_0$-martensite. Stabilization of detwinned $L1_0$-martensite leads to a TWSME with wide hysteresis and narrow intervals (explosive behaviour). Conversely, upon stabilization of the twinned $L1_0$-martensite, the TWSME curves with narrow hysteresis and wide intervals were obtained [23,24]. In the present work, various types of TWSME curves were obtained in quenched and heterophase single crystals, although in both cases only the twinned $L1_0$-martensite was stabilized during SIM-aging (upon compression along the [001] direction [24]). In the heterophase single crystals, where particles were precipitated only before SIM-aging, the TWSME curves conform to this classification. The TWSME curves obtained after SIM-aging with simultaneous particle precipitation do not conform to this classification. This feature is caused by ω-phase particles, which precipitated in oriented $L1_0$-martensite. The reason why the particles change the martensite morphology in this way, and the mechanism of MT, requires further investigation.

The temperature of oriented martensite formation M_S^* strongly depends on the SIM-aging temperature and the initial state. In the quenched single crystals, the SIM-aging is conducted only at temperatures above the ω-phase particle precipitation temperature, $T_{SIM} > T_\omega = 488$ K. SIM-aging caused the simultaneous precipitation of nanoscale ω-phase particles and the stabilization of martensite, which have opposing effects on M_S^*. Chemical stabilization of martensite reduces the free energy of the martensitic phase, increasing M_S^*. Dispersed particles act as obstacles to the movement of the interphase boundary and significantly enhance the martensite yield strength, which, conversely, leads to a decrease in M_S^*. In quenched single crystals after SIM-aging at 503 K, the TWSME occurs at $M_S^* = 324$ K, which is significantly lower than the initial $M_S^0 = 373$ K prior to SIM-aging. Therefore, the contribution to the change in MT temperature from the particles is greater than the contribution from martensite stabilization. The SIM-aging temperature increases to 533 K, the M_S^* temperature rises to 373 K and becomes equal to M_S^0. It can be assumed that the contribution of chemical martensite stabilization to the change in M_S^* increases. A similar case was observed in [8] on $Ni_{49}Fe_{18}Ga_{27}Co_6$ single crystals, where an increase in SIM-aging stress and time led to a greater shift in M_S^* due to a greater reduction in the energy of the martensitic phase.

In the pre-aged heterophase single crystals, which contain nanoscale particles of the ω-phase prior to SIM-aging, the MT temperature, $M_S^0 = 305$ K, is lower than in the quenched single crystals, where $M_S^0 = 373$ K. This is due to the precipitation of nanoscale ω-phase particles and was discussed in detail in [11]. In the heterophase single crystals, during SIM-aging at 398–533 K, no precipitation of ω-phase particles occurred; and, only chemical martensite stabilization took place. Therefore, the M_S^* temperature during the subsequent TWSME always increases relative to the initial M_S^0 (Figs. 4, 5). An increase in the SIM-aging temperature T_{SIM} from 398 to 533 K leads to a significant increase in M_S^* from 323 to 417 K (by more than 100 K relative to the initial state).

Thus, in the quenched and heterophase single crystals, the high-temperature TWSME was obtained (Fig. 5, bold curves, $T_{SIM} = 533$ K), which arises due to the chemical stabilization of martensite by SIM-aging under identical conditions (533 K, 500 MPa, 1 h). Both structural states contain nanoscale particles of the ω-phase, which formed during aging at temperatures of 523–533 K for 1 h. However, a significant difference between the two states lies in the structure in which the ω-phase particles formed.

In the quenched single crystals, ω-phase particles appeared in the oriented stress-induced $L1_0$-martensite, whereas in the heterophase single crystals, ω-phase particles appeared in the stress-free $L2_1$-austenite prior to SIM-aging. The mechanism for the ω-phase formation in a body-centered cubic matrix is well established. It involves the collapse of the {111} planes of the body-centered cubic phase [25–27]. The a thermal ω-phase results from a purely structural instability in the high-temperature phase, whilst the isothermal ω phase results from concurrent compositional and structural instabilities. In our previous article [28], it was shown for alloys of similar composition that low-temperature aging at 573 K results in the precipitation of particles with an ordered trigonal ω″ structure. They had lattice parameters $a_{\omega''} = \sqrt{2}a_{B2}$=0.4073 nm, $c_{\omega''} = \sqrt{3}a_{B2}$ =0.4988nm and orientation relations with $L2_1$-phase of $\langle 110\rangle_{L21} \parallel \langle 11\bar{2}0\rangle_{\omega''}$ and $\{111\}_{L21} \parallel (0001)_{\omega''}$. Similar particles have been observed in alloys [29–31]. The mechanism for the ω-phase

formation in the tetragonal structure is unknown. The precipitation of particles in tetragonal $L1_0$-martensite affects the mechanism of ω-phase formation and the orientation relationships with the matrix, and requires further investigation.

Conclusion

In the heterophase $Ni_{47.5}Fe_{15}Ga_{27.5}Co_{10}$ single crystals, in which nanoscale ω-phase particles were precipitated in the austenitic $L2_1$-phase before SIM-aging, the optimal parameters of the TWSME were demonstrated. The SIM-aging induced the TWSME with narrow thermal hysteresis (15–30 K) and allowed control of the M_S^* temperature in wide interval from 323 to 417 K. In contrast, the quenched single crystals, where nanoscale ω-phase particles were precipitated in oriented $L1_0$-martensite during SIM-aging, demonstrated the TWSME with a wide thermal hysteresis (45–60 K). The M_S^* temperature changed in a narrower interval from 324 to 373 K. The reversible strain of TWSME is 3.7–4 % and practically independent of the initial state.

CRediT authorship contribution statement

Ekaterina E. Timofeeva: writing – review & editing, writing – original draft; conceptualization; supervision; **Elena Yu. Panchenko**: writing – review & editing, conceptualization; **Nikita Yu. Surikov**: investigation; data curation; **Maria V. Zherdeva**: investigation; data curation; **Yury I. Chumlyakov**: supervision; writing – review & editing.

Conflict of interest

The authors declare that they have no conflict of interest.

References

1. Beke DL, Azim AA. On aging of stress induced martensite for production of high temperature shape memory alloys -Why SIM aging was not observed in NiTi? *Intermetallics.* 2026;188: 109028.
2. Wang Y, Jing T, Peng H, He W, Yan J, Wang S, Li N, Wen Y. Re-examination of martensitic stabilization in Cu-based shape memory alloys Part II. Key factors determining occurrence of martensitic stabilization in Cu-based alloys. *Journal of Alloys and Compounds.* 2022;915(15): 165401.
3. Shcherbakov AA, Vasin RN, Balagurov AM, Khovaylo V, Golovin IS Phase transformations and martensite stabilization in $Ni_{2.36}Mn_{0.64}Ga$ high-temperature shape memory alloy. *Defect and Diffusion Forum.* 2023;429: 117–126.
4. Otsuka K, Ren X. Mechanism of martensite aging effects and new aspects. *Materials Science and Engineering A.* 2001;312(1–2): 207–218.
5. Cingolani E, Stalmans R, Van Humbeeck J, Ahlers M. Influence of thermal treatments on the long range order and the two way shape memory effect induced by stabilization in Cu-Al-Be single crystals. *Materials Science and Engineering A.* 1999;268(1-2): 109–115.
6. Belyaev S, Resnina N, Iaparova E, Ivanova A, Rakhimov T, Andreev V. Influence of chemical composition of NiTi alloy on the martensite stabilization effect. *Materials Science and Engineering A.* 2019;787: 1365–1371.
7. Kustov S, Pons J, Cesari E, Van Humbeeck J. Chemical and mechanical stabilization of martensite. *Acta Materialia.* 2004;52(15): 4547–4559.
8. Tokhmetova AB, Larchenkova NG, Panchenko EYu, Chumlyakov YuI. The influence of compressive-stress-induced martensite aging on the two-way shape memory effect in single crystals of $Ni_{49}Fe_{18}Ga_{27}Co_6$ ferromagnetic alloy. *Technical Physics Letters.* 2020;46: 621–624.

9. Volkov AE, Belyaev FS, Volkova NA, Vukolov EA, Evard ME, Rebrov TV. The effect of martensite stabilization in titanium nickelide after various methods of pre-deformation: simulation with a single set of constants. *Materials Physics and Mechanics.* 2024;52(4): 91–99.
10. Resnina NN, Belyaev SP, Bazlov AI, Sibirev AV, Ponikarova IV, Trofimova ME, Ivanov AM, Bikbaev RM. Thermal cycling stability of the martensitic transformation in $Ti_{40.7}Hf_{9.5}Ni_{49.8-x}Cu_x$ (x = 1, 5 or 10 at. %) cast alloys. *Materials Physics and Mechanics.* 2025;53(1): 57–67.
11. Timofeeva EE, Panchenko EY, Surikov NY, Volochaev MN, Chumlyakov YI. The effect of ω-phase precipitation on thermal- and stressinduced martensitic transformations in $Ni_{47.5}Fe_{15}Ga_{27.5}Co_{10}$ single crystals. *Applied Physics Letters.* 2026; 128(11): 111903.
12. Chen H, Wang Y, Nie Z, Li R, Cong D, Liu W, Ye F, Liu Y, Cao P, Tian F, Shen X, Yu R, Vitos L, Zhang M, Li S, Zhang X, Zheng H, Mitchell JF, Ren Y. Unprecedented non-hysteretic superelasticity of [001]-oriented NiCoFeGa single crystals. *Nature Materials.* 2020;19: 712.
13. Banerjee A. *Advances in Physical Metallurgy.* CRC Press; 2023.
14. Masoumi F, Shahriari D, Jahazi M, Cormier J, Devaux A. Kinetics and mechanisms of γ′ reprecipitation in a Ni-based superalloy. *Scientific Reports.* 2016;6: 28650.
15. Hornbogen E. The effect of variables on martensitic transformation temperatures. *Acta Metallurgica et Materialia.* 1985;33(4): 595–601.
16. Panchenko EYu, Chumlyakov YuI, Kireeva IV, Ovsyannikov AV, Sehitoglu H, Karaman I, Maier HJ. Effect of disperse Ti_3Ni_4 particles on the martensitic transformations in titanium nickelide single crystals. *Physics of Metals And Metallography.* 2008;106(6): 577–589.
17. Sehitoglu H, Wang J, Maier HJ. Transformation and slip behavior of Ni_2FeGa. *International Journal of Plasticity.* 2012;39: 61–74.
18. Panchenko EYu, Timofeeva EE, Larchenkova NG, Chumlyakov YuI, Tagiltsev AI, Maier HJ, Gerstein G. Two-way shape memory effect under multi-cycles in [001]-oriented $Ni_{49}Fe_{18}Ga_{27}Co_6$ single crystal. *Materials Science & Engineering A.* 2017;706: 95–103.
19. Ortinh J, Planes A. Thermodynamic analysis of thermal measurements in thermoelastic martensitic transformation. *Acta Metallurgica.* 1988;36(8): 1873–1889.
20. Beke DL, Daryczi L, Elrasasi TY. Determination of Elastic and Dissipative Energy Contributions to Martensitic Phase Transformation in Shape Memory Alloys. In: Fernandes FMB. (Ed.) *Shape Memory Alloys - Processing, Characterization and Applications.* IntechOpen; 2013. p.167–196.
21. Nikolaev VI, Timashov RB, Pulnev SA, Guzilova LI, Butenko PN, Stepanov SI. Jumping at strain recovery in shape memory Cu-Al-Ni single crystals. *Materials Physics and Mechanics.* 2021;47(1): 59–64.
22. Mohd J, Leary M, Subic A, Gibson MA. A review of shape memory alloy research, applications and opportunities. *Materials and Design.* 2014;56: 1078–1113.
23. Samy NM, Daróczi L, Tóth LZ, Panchenko E, Chumlyakov Y, Surikov N, Beke DL. Effect of stress-induced martensite stabilization on acoustic emission characteristics and the entropy of martensitic transformation in shape memory $Ni_{51}Fe_{18}Ga_{27}Co_4$ single crystal. *Metals.* 2020;10(4): 534.
24. Eftifeeva A, Panchenko E, Yanushonite E, Tagiltsev A, Ryzhakova V, Steshenko I, Chumlyakov Y. Orientation dependence of stress-induced martensite stabilization and two-way shape memory effect in CoNiAlFe single crystals. *Journal of Alloys and Compounds.* 2026;1059: 187137.
25. Sinkler W, Luzzi DE. An electron diffraction investigation of the diffuse ω structure in quenched Ti-3d transition metal alloys. *Acta Metallurgica et Materialia.* 1994;42(4): 1249–1260.
26. Goel L, Ghosh PS, Mani Krishna KV, Arya A, Tewari R. A study on the evolution of ω-phase in Zr-20Nb alloy under the influence of electron irradiation. *Journal of Alloys and Compounds.* 2022;904: 163968.
27. Devaraj A, Nag S, Srinivasan R, Williams REA, Banerjee S, Banerjee R, Fraser HL. Experimental evidence of concurrent compositional and structural instabilities leading to ω precipitation in titanium–molybdenum alloys. *Acta Materialia.* 2012;60(2): 596–609.
28. Timofeeva EE, Panchenko EY, Surikov NY, Volochaev MN, Chumlyakov YI. The effect of ω-phase precipitation on thermal- and stress-induced martensitic transformations in $Ni_{47.5}Fe_{15}Ga_{27.5}Co_{10}$ single crystals. *Applied Physics Letters.* 2026;128: 111903.
29. Shao G, Tsakiropoulos P. On the ω phase formation in Cr–Al and Ti–Al–Cr alloys. *Acta Materialia.* 2000;48(14): 3671.
30. Song L, Zhang LQ, Xu XJ, Sun J, Lin JP. Omega phase in as-cast high-Nb-containing TiAl alloy. *Scripta Materialia.* 2013;68: 929–932.
31. Goel L, Ghosh PS, Mani Krishna KV, Arya A, Tewari R. A study on the evolution of ω-phase in Zr-20Nb alloy under the influence of electron irradiation. *Journal of Alloys and Compounds.* 2022;904: 163968.